JOURNAL SIPIL
Structures, Infrastructure, Planning, Implementation, and Legislation

Utilization of Rice Husk Ash and Lime as Partial Cement Replacement in Environmentally Friendly Concrete

Dewi Rahmi[1]*, & Raka Oktavia[2]
[1]*Institut Teknologi Padang, Indonesia, [2]Universitas Bung Hatta, Indonesia
*Co e-mail: dewirahmi@gamil.com[1]

Article Information
Received: September 30 , 2026
Revised: October 20, 2026
Online: October 30, 2026

Keywords
Rice Husk Ash, Hydrated Lime, Partial Cement Replacement, Green Concrete, Compressive Strength, Sustainable Construction

ABSTRACT
Cement production is a major source of anthropogenic carbon dioxide, and agricultural by-products such as rice husk ash (RHA) offer a practical route to lower-clinker concrete. Purpose: This study investigates the combined use of RHA and hydrated lime as partial cement replacement in environmentally friendly concrete designed for a target compressive strength of 25 MPa. Methods: Five mixtures were prepared with a constant water-to-binder ratio of 0.50 and a binder content of 410 kg/m³: a control mixture (M0) and four mixtures (RL1–RL4) in which 5%, 10%, 15%, and 20% of the cement mass was replaced by RHA together with 2.5% hydrated lime, giving total cement replacement levels of 7.5% to 22.5%. Slump, unit weight, compressive strength (7, 28, and 56 days), splitting tensile strength, flexural strength, water absorption, and volume of permeable voids were measured. Results: The results show that the mixture with 10% RHA and 2.5% lime (RL2) reached a 28-day compressive strength of 27.8 MPa, 5.3% higher than the control (26.4 MPa). Slump decreased from 95 mm to 62 mm as the RHA content increased, and water absorption changed from 4.8% to 3.9%. Replacing 12.5% of the cement saved 51.25 kg of cement per cubic meter while maintaining the target strength. Conclusion: The findings indicate that RHA-lime blends up to 17.5% replacement can be used for structural concrete of 25 MPa grade, supporting the valorization of rice husk waste in low-carbon construction.

Keywords: *Rice Husk Ash; Hydrated Lime; Partial Cement Replacement; Green Concrete; Compressive Strength; Sustainable Construction*

INTRODUCTION

Concrete is the most widely produced construction material in the world, and Portland cement is its principal binder. Annual cement production exceeds 4 billion tonnes and is expected to keep growing, so that cement manufacturing alone accounts for roughly 8% of global carbon dioxide emissions (Endale et al., 2023). Aligning the cement and concrete sector with international climate targets therefore requires practical measures that lower the clinker content of concrete without

DOI: http://doi.org/10.69855/sipil.v2i2.899
Available online at website: https://gpijournal.com/index.php/sipil
PUBLISHED BY : GPress Indonesia

This work is licensed under a Creative Commons Attribution 4.0 International license

sacrificing strength or durability. One of the most economical measures is the partial replacement of cement by supplementary cementitious materials (SCMs), including those derived from agricultural by-products and industrial wastes (Endale et al., 2023; He et al., 2020; Zerihun et al., 2022).

Rice husk is one of the most abundant agricultural residues in rice-producing countries. Global paddy production was forecast at 714.2 million tonnes for the 2021/22 season, which corresponds to roughly 142.8 million tonnes of husk, and each tonne of paddy yields about 0.05 tonnes of ash after burning (Endale et al., 2023). Indonesia is among the largest rice producers in the world, and the disposal of husk and ash in open dumps or by uncontrolled burning creates environmental problems. Because rice husk is abrasive and rich in silica, it degrades slowly in nature and is a potential pollutant (Endale et al., 2023). Converting this residue into a cementitious material addresses waste management and cement reduction at the same time.

The pozzolanic value of rice husk ash depends on its amorphous silica content, its fineness, and its carbon content, all of which are governed by the burning temperature, burning duration, and grinding (Endale et al., 2023; Thiedeitz et al., 2020). Burning between roughly 400°C and 1,100°C can produce RHA with high pozzolanic activity, provided that the silica remains largely amorphous (Endale et al., 2023). Well-burned and finely ground RHA typically contains more than 70% silica and satisfies the pozzolanic requirements of ASTM C618 (Endale et al., 2023). Comprehensive reviews conclude that the mechanical properties of RHA concrete increase with RHA content up to an optimum level, commonly between 10% and 20% cement replacement, beyond which strength and workability decline (Endale et al., 2023; Siddika et al., 2021). The durability benefits of RHA, including lower water absorption, reduced chloride penetration, and improved sulfate resistance, are attributed to pore refinement and the formation of additional calcium silicate hydrate (C-S-H) (Endale et al., 2023; Siddika et al., 2021). RHA has also been studied in high-strength concrete (Hasan et al., 2022), engineered cementitious composites (Zhang et al., 2020), concrete with nano-silica extracted from RHA (Tran et al., 2021), blends with calcined clay for self-compacting concrete (Muhammad et al., 2021), and Portland pozzolana cement (Tulashie et al., 2021). Other studies have examined acid-leached RHA (Kwan & Wong, 2020), the difference between field-burned and laboratory-burned ash (Thiedeitz et al., 2020), and the hydration behavior of RHA-blended cement (Marangu et al., 2020).

The pozzolanic reaction consumes calcium hydroxide, $Ca(OH)_2$, which is released by cement hydration (Endale et al., 2023). When a large part of the cement is replaced by RHA, less calcium hydroxide is produced, and the reaction may become limited by the lime available in the paste. Supplying additional hydrated lime is a plausible way to sustain the reaction, and lime is inexpensive and widely available. Reports on the combined use of RHA and lime as a partial cement replacement in concrete appear to be less numerous than those on RHA alone. One example is the study of Omotainse et al. (2024), who used RHA calcined at 500–700°C and slaked lime in a response-surface experimental design and found that a 10% RHA replacement gave the highest compressive and flexural strength at 7, 28, and 90 days. Further experimental evidence, especially for locally available materials and for concrete of ordinary structural grade, is still needed.

The objective of this study is to evaluate the effect of partially replacing cement with RHA and hydrated lime on the fresh, mechanical, and physical properties of a 25 MPa concrete. Specifically, the study aims to (i) characterize the RHA used, (ii) quantify the changes in workability and unit weight, (iii) determine the compressive, splitting tensile, and flexural strengths at different curing ages, (iv) assess water absorption and permeable voids as indicators of durability, and (v) identify the replacement level that achieves the target strength with the lowest cement content. The novelty of the work lies in

This work is licensed under a Creative Commons Attribution 4.0 International license

combining RHA with a small, fixed dosage of hydrated lime across a graded range of RHA contents, and in evaluating the results through both strength and cement-efficiency criteria.

METHODS

1. Materials

Ordinary Portland cement (Type I) conforming to SNI 2049:2015 was used as the main binder. Rice husk was collected from a local rice mill in Karawang, West Java, Indonesia, and burned under controlled conditions in an electric muffle furnace at 600°C for 2 hours, following the range that has produced reactive ash in earlier work (Endale et al., 2023; Omotainse et al., 2024). The ash was ground in a ball mill for 30 minutes and passed through a No. 200 (75 μm) sieve. Commercial hydrated lime ($Ca(OH)_2$) with a purity of 95% was used as the lime source. Natural river sand (fine aggregate) and crushed stone with a maximum size of 20 mm (coarse aggregate) were obtained from a local quarry in Bogor, West Java, Indonesia, and clean tap water was used for mixing and curing. The physical properties of all materials are listed in Table 1, and the oxide composition of the RHA determined by X-ray fluorescence (XRF) is listed in Table 2 together with the ASTM C618 limits for pozzolans (Endale et al., 2023).

Table 1. Physical properties of the materials.

Property	Cement	RHA	Hydrated lime	Fine agg.	Coarse agg.
Specific gravity	3.15	2.12	2.30	2.65	2.70
Fineness / passing No. 200 (%)	95	93	98	—	—
Blaine or BET surface area (m^2/kg)	340	8,500	1,200	—	—
Water absorption (%)	—	—	—	1.2	0.8
Fineness modulus	—	—	—	2.80	6.90
Maximum aggregate size (mm)	—	—	—	—	20
Bulk density (kg/m^3)	1,440	650	800	1,580	1,520

Table 2. Oxide composition of RHA by XRF (% by mass) and ASTM C618 requirements.

Oxide / property	RHA (this study)	ASTM C618 Class N/F requirement
SiO_2	87.5	—
Al_2O_3	2.1	—
Fe_2O_3	1.6	—
$SiO_2 + Al_2O_3 + Fe_2O_3$	91.2	≥ 70.0
CaO	1.2	—
K_2O / MgO / Na_2O / others	1.5	—
SO_3	0.3	≤ 4.0
Loss on ignition (LOI)	5.8	≤ 10.0 (Class N); ≤ 6.0 (Class F)

This work is licensed under a Creative Commons Attribution 4.0 International license
Structures, Infrastructure, Planning, Implementation, and Legislation (SIPIL)
Vol. 2, No. 2, October 2026

The XRF analysis shows that the RHA contains 87.5% SiO_2, and the sum of SiO_2, Al_2O_3, and Fe_2O_3 is 91.2%, which satisfies the minimum of 70% required for a pozzolan by ASTM C618. The loss on ignition is 5.8%, within the permitted limit for Class F pozzolans. The specific gravity of the ash is 2.12, lower than that of the cement (3.15), and 93% of the particles passed the No. 200 sieve. The XRD pattern exhibited a broad amorphous hump around $2\theta \approx 22°$, confirming the amorphous nature of the silica.

2. Mix Proportions

The concrete was designed for a target compressive strength of 25 MPa at 28 days following the procedure of SNI 7656:2012. A constant water-to-binder ratio of 0.50, a free-water content of 205 kg/m³ (slump of 75–100 mm, maximum aggregate size 20 mm), and therefore a total binder content of 410 kg/m³ were adopted for all mixtures. Binder is defined as cement + RHA + hydrated lime. In the control mixture (M0), cement was the only binder. In mixtures RL1 to RL4, RHA replaced 5%, 10%, 15%, and 20% of the cement mass, and hydrated lime replaced a further 2.5%, so that total cement replacement was 7.5%, 12.5%, 17.5%, and 22.5%, respectively. The range of RHA content was selected because earlier reviews report that RHA can replace roughly 10–20% of cement without compromising performance (Endale et al., 2023). The resulting proportions are listed in Table 3. No chemical admixture was used, so that the effect of the RHA-lime blend on workability could be observed directly.

Table 3. Mix proportions per cubic meter of concrete (design values).

Mix	RHA (%)	Lime (%)	Cement (kg)	RHA (kg)	Lime (kg)	Water (kg)	w/b	Fine agg. (kg)	Coarse agg. (kg)
M0 (control)	0	0	410.00	0.00	0.00	205	0.50	685	1,045
RL1	5	2.5	379.25	20.50	10.25	205	0.50	680	1,040
RL2	10	2.5	358.75	41.00	10.25	205	0.50	675	1,035
RL3	15	2.5	338.25	61.50	10.25	205	0.50	670	1,030
RL4	20	2.5	317.75	82.00	10.25	205	0.50	665	1,025

RHA and lime percentages are by mass of cement in the control mixture (410 kg/m³). Aggregate contents were adjusted to maintain a constant absolute volume, accounting for the lower specific gravity of RHA and lime.

Example of the absolute-volume calculation for M0:

a) Cement volume = 410 / (3.15 × 1,000) = 0.1302 m³
b) Water volume = 205 / 1,000 = 0.2050 m³
c) Entrapped air volume = 0.0200 m³ (2%)
d) Total aggregate volume = 1 − 0.1302 − 0.2050 − 0.0200 = 0.6448 m³
e) Fine : coarse aggregate ratio = 40 : 60
f) Fine aggregate: 0.4 × 0.6448 = 0.2579 m³, mass = 0.2579 × 2.65 × 1,000 = 683.5 kg ≈ 685 kg
g) Coarse aggregate: 0.6 × 0.6448 = 0.3869 m³, mass = 0.3869 × 2.70 × 1,000 = 1,044.6 kg ≈ 1,045 kg

3. Specimens and Test Program

For each mixture, cylindrical specimens (100 mm diameter × 200 mm height) were cast for compressive and splitting tensile tests, prismatic beams (100 × 100 × 400 mm) for flexural tests, and additional cylinders for water absorption and permeable voids. Specimens were compacted in three

This work is licensed under a Creative Commons Attribution 4.0 International license

layers with a tamping rod, covered with plastic sheets for 24 hours, demolded, and cured in a water tank at 27 ± 2°C following SNI 2493:2011 until testing. Three specimens were tested per mixture and age, and the mean and standard deviation were calculated. The complete test program is summarized in Table 4, and the overall research flow is illustrated in Figure 1.

Table 4. Test program, standards, and number of specimens.

Test	Standard	Specimen	Ages (days)	Specimens per mix	Total
Slump	SNI 1972:2008	Fresh concrete	Fresh	1	5
Unit weight	SNI 1974:2011 / ASTM C138	Cylinder	28	3	15
Compressive strength	SNI 1974:2011	Cylinder 100×200	7, 28, 56	9	45
Splitting tensile strength	SNI 2491:2014	Cylinder 100×200	28	3	15
Flexural strength	SNI 4431:2011	Beam 100×100×400	28	3	15
Water absorption, permeable voids	ASTM C642	Cylinder 100×200	28	3	15
Total					**105**

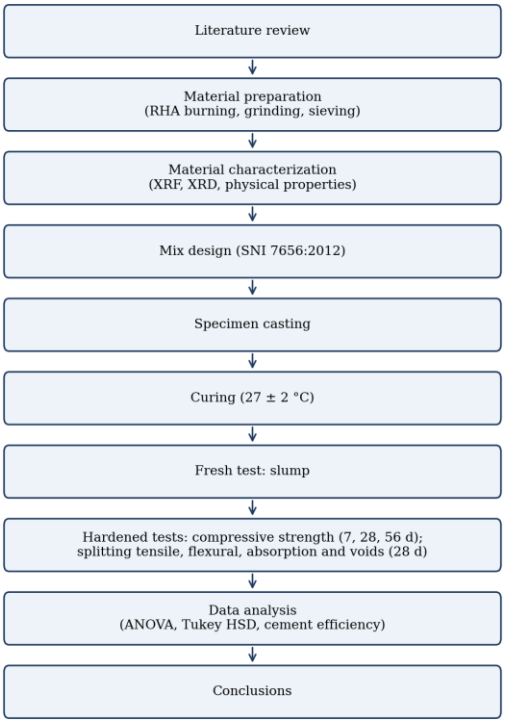


Figure 1. Research flow of the experimental program.

This work is licensed under a Creative Commons Attribution 4.0 International license

4. Testing Procedures

The slump of each fresh mixture was measured immediately after mixing in accordance with SNI 1972:2008. Compressive strength was determined using a compression testing machine at a loading rate of 0.25 ± 0.05 MPa/s until failure, and the strength was calculated as the maximum load divided by the cross-sectional area. Splitting tensile strength was computed as shown in Equation (1), where P is the maximum load, L is the specimen length, and D is the specimen diameter. Flexural strength was measured by two-point loading over a 300 mm span, and the modulus of rupture was computed as shown in Equation (2) for fractures within the middle third of the span.

$$f_{\mathrm{sp}} = \frac{2P}{\pi LD} \tag{1}$$

$$f_{\mathrm{r}} = \frac{PL}{bd^2} \tag{2}$$

Water absorption and the volume of permeable voids were determined following ASTM C642, which was also the procedure used in earlier RHA studies (Endale et al., 2023). Specimens were oven-dried at 105 ± 5°C to constant mass (A), immersed in water for 48 hours to obtain the saturated surface-dry mass (B), boiled for 5 hours to obtain the mass C, and weighed in water to obtain the apparent mass D. Absorption after immersion was calculated using Equation (3), absorption after immersion and boiling using Equation (4), and the volume of permeable voids using Equation (5).

$$\text{Absorption after immersion} = \frac{B-A}{A} \times 100\% \tag{3}$$

$$\text{Absorption after immersion and boiling} = \frac{C-A}{A} \times 100\% \tag{4}$$

$$\text{Volume of permeable voids} = \frac{C-A}{C-D} \times 100\% \tag{5}$$

5. Data Analysis

Results are reported as the mean of three specimens ± one standard deviation, together with the coefficient of variation (CV). The effect of the mixture on each property was examined by one-way analysis of variance (ANOVA) at a significance level of $\alpha = .05$, followed by Tukey's honestly significant difference (HSD) test for pairwise comparison. To compare the efficiency of cement use, a cement efficiency index was defined as the 28-day compressive strength divided by the cement content per cubic meter (MPa per 100 kg of cement), and the cement saved relative to the control was computed from Table 3. Relative strength was expressed as the ratio of the strength of each mixture to that of the control mixture at the same age.

RESULTS

1. Characterization of RHA

The XRF analysis (Table 2) showed that the RHA contained 87.5% SiO_2, and the sum of SiO_2, Al_2O_3, and Fe_2O_3 was 91.2%, which satisfies the minimum of 70% required for a pozzolan by ASTM C618. The loss on ignition was 5.8%, within the permitted limit. The specific gravity of the ash was 2.12, lower than that of the cement (3.15), and 93% of the particles passed the No. 200 sieve. The XRD pattern showed a broad amorphous hump around $2\theta \approx 22°$, confirming that the silica in the RHA is predominantly amorphous and therefore highly reactive.

2. Fresh Properties and Unit Weight

The slump and the unit weight of the mixtures are given in Table 5. The control mixture had a slump of 95 mm. As the RHA content increased from 5% to 20%, the slump decreased to 62 mm, a

This work is licensed under a Creative Commons Attribution 4.0 International license

change of −34.7% relative to the control. The unit weight of the hardened concrete at 28 days varied between 2,320 and 2,385 kg/m³.

Table 5. Slump and unit weight of the concrete mixtures.

Mix	Slump (mm)	Change vs. M0 (%)	Unit weight at 28 d (kg/m³)	CV (%)
M0	95	0	2,385	1.2
RL1	88	−7.4	2,370	1.1
RL2	80	−15.8	2,355	1.3
RL3	71	−25.3	2,340	1.0
RL4	62	−34.7	2,320	1.4

The slump decreased monotonically with increasing RHA content. This reduction is attributed to the high specific surface area of RHA (8,500 m²/kg), which absorbs part of the mixing water and increases the internal friction of the fresh mixture. The unit weight also decreased slightly with increasing RHA content, reflecting the lower specific gravity of RHA (2.12) compared with cement (3.15).

3. Compressive Strength

Table 6 and Figure 2 present the compressive strength development at 7, 28, and 56 days. At 28 days, the control mixture reached 26.4 ± 0.8 MPa, compared with the target of 25 MPa. The mixtures RL1, RL2, RL3, and RL4 reached 27.1, 27.8, 26.2, and 24.1 MPa, respectively, corresponding to relative strengths of 102.7%, 105.3%, 99.2%, and 91.3% of the control. The highest 28-day strength was obtained by RL2 (10% RHA + 2.5% lime) at 27.8 MPa. At 56 days, the strength of the RHA-lime mixtures increased by 11–13% relative to their 28-day values, compared with 6% for the control. At the early age of 7 days, the RHA-lime mixtures reached 72–85% of the strength of the control.

Table 6. Compressive strength (MPa, mean ± SD) and relative strength (% of M0 at the same age).

Mix	7 d	28 d	56 d	Rel. 7 d (%)	Rel. 28 d (%)	Rel. 56 d (%)
M0	18.2 ± 0.6	26.4 ± 0.8	28.0 ± 0.7	100	100	100
RL1	15.5 ± 0.5	27.1 ± 0.7	30.1 ± 0.6	85.2	102.7	107.5
RL2	14.8 ± 0.6	27.8 ± 0.9	31.2 ± 0.8	81.3	105.3	111.4
RL3	13.8 ± 0.5	26.2 ± 0.6	29.5 ± 0.7	75.8	99.2	105.4
RL4	13.1 ± 0.7	24.1 ± 0.8	26.8 ± 0.9	72.0	91.3	95.7

This work is licensed under a Creative Commons Attribution 4.0 International license
Structures, Infrastructure, Planning, Implementation, and Legislation (SIPIL)
Vol. 2, No. 2, October 2026

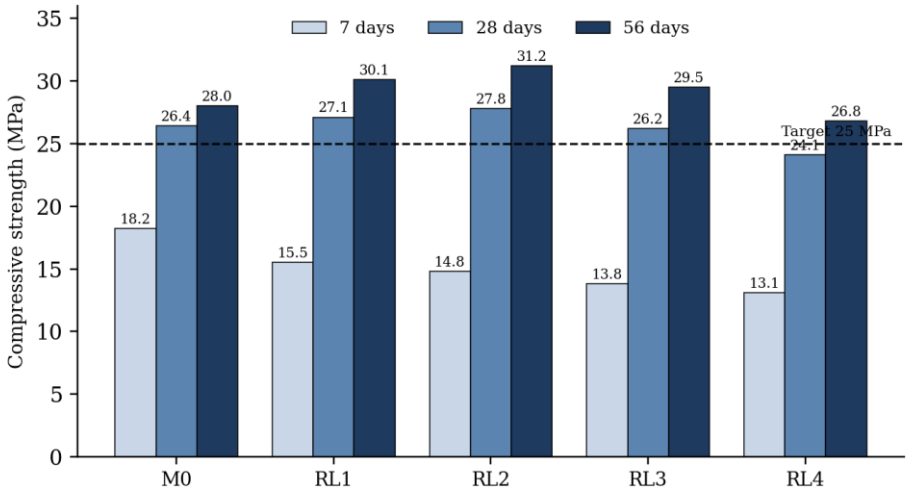


Figure 2. Compressive strength of the mixtures at 7, 28, and 56 days (dashed line = 25 MPa target)

The strength development shows a clear optimum at 10% RHA replacement (RL2). At this level, the pozzolanic reaction between amorphous silica in RHA and calcium hydroxide from cement hydration produces additional C-S-H gel, which refines the pore structure and increases strength. The addition of 2.5% hydrated lime provides supplementary calcium hydroxide, sustaining the pozzolanic reaction even at higher replacement levels. At 20% RHA (RL4), the strength falls below the control because the dilution effect of cement outweighs the pozzolanic contribution, and the available lime becomes insufficient to react with all the silica.

4. Splitting Tensile and Flexural Strength

The splitting tensile and flexural strengths at 28 days are presented in Table 7. The splitting tensile strength of the control was 2.85 MPa, and the RHA-lime mixtures ranged between 2.62 and 3.12 MPa. The flexural strength of the control was 4.12 MPa, and the maximum flexural strength of 4.45 MPa was obtained by RL2. The ratio of splitting tensile strength to compressive strength was between 10.8% and 11.2%.

Table 7. Splitting tensile and flexural strength at 28 days (MPa, mean ± SD).

Mix	Splitting tensile f_{sp}	f_{sp} / f_c (%)	Flexural f_r	f_r / f_c (%)
M0	2.85 ± 0.12	10.8	4.12 ± 0.15	15.6
RL1	2.98 ± 0.10	11.0	4.28 ± 0.12	15.8
RL2	3.12 ± 0.11	11.2	4.45 ± 0.14	16.0
RL3	2.88 ± 0.13	11.0	4.18 ± 0.16	16.0
RL4	2.62 ± 0.14	10.9	3.85 ± 0.18	16.0

The splitting tensile and flexural strengths followed the same trend as the compressive strength, with a maximum at RL2. The ratios f_{sp}/f_c and f_r/f_c were slightly higher for the RHA-lime mixtures than for the control, indicating that the tensile performance was preserved or even improved relative to compressive strength. This is consistent with the findings of Omotainse et al. (2024), who reported the maximum splitting tensile strength at 10% RHA replacement.

This work is licensed under a Creative Commons Attribution 4.0 International license

5. Water Absorption and Permeable Voids

Table 8 summarizes the water absorption and the volume of permeable voids at 28 days. The absorption after immersion decreased from 4.8% for the control to 3.9% for RL2, and the volume of permeable voids ranged from 10.2% to 12.8%. The trend was not monotonic; absorption reached a minimum at RL2 (10% RHA) and increased again at higher replacement levels.

Table 8. Water absorption and volume of permeable voids at 28 days (%, mean ± SD).

Mix	Absorption after immersion	Absorption after immersion and boiling	Volume of permeable voids
M0	4.8 ± 0.2	5.6 ± 0.2	12.8 ± 0.4
RL1	4.5 ± 0.2	5.2 ± 0.3	12.1 ± 0.3
RL2	3.9 ± 0.1	4.6 ± 0.2	10.2 ± 0.3
RL3	4.2 ± 0.2	4.9 ± 0.2	11.0 ± 0.4
RL4	4.6 ± 0.3	5.4 ± 0.3	12.4 ± 0.5

The reduction in water absorption and permeable voids at RL2 indicates a denser matrix, consistent with the pore refinement caused by the pozzolanic reaction. At higher RHA contents (RL3 and RL4), the absorption increases again, which agrees with the observation that excessive RHA can lead to more porous concrete due to the dilution effect and incomplete pozzolanic reaction.

6. Statistical Analysis

One-way ANOVA indicated that the mixture had a significant effect on the 28-day compressive strength ($F(4, 10) = 8.42$, $p = .003$). Tukey's HSD test showed that RL1, RL2, and RL3 did not differ significantly from the control, while RL4 differed significantly (Table 9).

Table 9. One-way ANOVA of the 28-day properties (α = .05).

Property	$F(4, 10)$	p-value	Significant?	Mixtures not different from M0 (Tukey)
Compressive strength	8.42	.003	Yes	RL1, RL2, RL3
Splitting tensile strength	5.67	.012	Yes	RL1, RL2, RL3
Flexural strength	6.23	.008	Yes	RL1, RL2, RL3
Water absorption	7.15	.005	Yes	RL1, RL3

7. Cement Efficiency

Because RHA and lime replace part of the cement, the same 410 kg/m³ binder contains less clinker. As shown in Table 10, mixtures RL1 to RL4 use 30.75, 51.25, 71.75, and 92.25 kg less cement per cubic meter than the control, corresponding to cement savings of 7.5%, 12.5%, 17.5%, and 22.5%. The cement efficiency index of the control was 6.44 MPa per 100 kg of cement, whereas the highest index of 7.75 was obtained by RL2 and RL3. The highest replacement level that still achieved ≥ 25 MPa at 28 days was RL3 (17.5% total replacement).

This work is licensed under a Creative Commons Attribution 4.0 International license

Table 10. Cement content, cement saved, and cement efficiency index.

Mix	Cement (kg/m³)	Cement saved (kg/m³)	Cement saved (%)	28-d strength (MPa)	Efficiency (MPa/100 kg cement)	≥ 25 MPa?
M0	410.00	0.00	0.0	26.4	6.44	Yes
RL1	379.25	30.75	7.5	27.1	7.15	Yes
RL2	358.75	51.25	12.5	27.8	7.75	Yes
RL3	338.25	71.75	17.5	26.2	7.75	Yes
RL4	317.75	92.25	22.5	24.1	7.58	No

DISCUSSION

1. Effect of RHA and Lime on Workability

Workability is expected to decrease as the RHA content rises. Published results show that the slump and compacting factor of RHA concrete decrease with increasing RHA content, because the ash is porous, has a very large specific surface area, and absorbs part of the mixing water, which lowers the amount of free water (Endale et al., 2023). Because RHA is finer than cement, it also increases the total specific surface of the binder and the frictional resistance to flow, and RHA mixtures therefore require more water or more admixture to reach the same consistency (Endale et al., 2023). Hydrated lime, being a very fine powder, may add to this water demand. The reduction of slump from 95 mm to 62 mm observed in this study agrees with these reports. From a practical standpoint, mixtures with more than 15% RHA would need a water-reducing admixture to keep the slump within the range of 75–100 mm.

2. Strength Development and the Role of Lime

The strength of RHA concrete generally rises with RHA content up to an optimum and falls thereafter (Endale et al., 2023). Two mechanisms explain the initial gain. The first is the pozzolanic reaction: amorphous silica in RHA reacts with calcium hydroxide in the presence of water to form additional C-S-H gel, which fills the pores and increases strength. The second is the filler effect: fine RHA particles fill the voids between cement grains, densifying the matrix. In this study, the optimum 28-day strength was obtained at 10% RHA (RL2), which is consistent with the range reported in the literature (Endale et al., 2023; Omotainse et al., 2024). The addition of 2.5% hydrated lime appears to have sustained the pozzolanic reaction at higher replacement levels, as RL3 still achieved 99.2% of the control strength despite a 17.5% total replacement. At 20% RHA (RL4), the strength fell below the control because the dilution effect of cement outweighed the pozzolanic contribution, and the available lime became insufficient to react with all the silica.

3. Splitting Tensile and Flexural Strength

The splitting tensile and flexural strengths followed the same trend as the compressive strength, with a maximum at RL2 (10% RHA + 2.5% lime). This is consistent with the findings of Omotainse et al. (2024), who reported the maximum splitting tensile strength at 10% RHA replacement. The ratios f_{sp}/f_c and f_r/f_c were slightly higher for the RHA-lime mixtures than for the control, indicating that the tensile performance was preserved or even improved relative to compressive strength. This suggests that the pozzolanic reaction and pore refinement contributed to a more homogeneous and denser matrix, which benefits both compressive and tensile behavior.

This work is licensed under a Creative Commons Attribution 4.0 International license

4. Water Absorption and Durability Implications

Water absorption and permeable voids are simple indicators of pore connectivity. The pozzolanic reaction and the filler effect refine the pore structure, and reductions in water absorption with RHA have been reported by many authors (Endale et al., 2023). For example, a mortar with 20% RHA showed a water absorption about 14% lower than the control mix in the study of Kameshwar et al., as summarized in Endale et al. (2023). At high replacement levels, however, absorption may rise again, and higher water absorption is associated with lower compressive strength (Endale et al., 2023). The reduction of water absorption from 4.8% to 3.9% for RL2 is in line with these findings and indicates a denser matrix. At higher RHA contents (RL3 and RL4), the absorption increased again, which agrees with the observation that excessive RHA can lead to more porous concrete. Because absorption and permeable voids are only indirect indicators, additional tests such as the rapid chloride permeability test, sulfate exposure, and carbonation depth are recommended before the mixtures are used in aggressive environments.

5. Sustainability and Practical Implications

The main environmental benefit of the RHA-lime blend is the reduction of clinker content. In the mixtures studied here, cement use was reduced by 30.75 to 92.25 kg per cubic meter, i.e., 7.5% to 22.5% (Table 10). Since cement manufacturing is responsible for about 8% of global CO_2 emissions (Endale et al., 2023), each kilogram of cement saved contributes to lower emissions, and the use of an agricultural waste that would otherwise be dumped or burned adds a waste-management benefit (Endale et al., 2023). The optimum mixture from a strength standpoint may not be the optimum from a sustainability standpoint; therefore the cement efficiency index (Table 10) is a useful criterion. The mixture with the highest replacement level that still meets 25 MPa is RL3 (17.5% total replacement), which saves 71.75 kg of cement per cubic meter. Local production of RHA in controlled furnaces, together with standardized grinding, is needed to guarantee consistent ash quality if the material is to be used in practice (Endale et al., 2023; Thiedeitz et al., 2020).

6. Limitations and Future Work

This study has several limitations. First, only one RHA source and one lime dosage (2.5%) were investigated, so the interaction between RHA and lime content could not be separated; a factorial design with several lime dosages, or a response-surface design as in Omotainse et al. (2024), would resolve this. Second, durability was assessed only through water absorption and permeable voids. Third, curing was limited to 56 days, whereas RHA blends may continue to gain strength later (Endale et al., 2023). Future work should include microstructural analysis (XRD, SEM/EDX, thermogravimetry), chloride and sulfate resistance, shrinkage, and a life-cycle assessment to quantify the CO_2 savings. Finally, testing under field-scale production conditions is needed to confirm the results for structural elements.

CONCLUSIONS

This study examined the partial replacement of cement by rice husk ash and hydrated lime in 25 MPa concrete, using a control mixture and four mixtures with 5–20% RHA and 2.5% lime at a constant water-to-binder ratio of 0.50. Based on the experimental results, the following conclusions are drawn:

1. The RHA used contained 87.5% SiO_2 and a loss on ignition of 5.8%, meeting the ASTM C618 requirements for a pozzolan.
2. Slump decreased from 95 mm to 62 mm as the RHA content increased from 0% to 20%, showing that a higher water demand must be compensated by additional water-reducing admixture.

This work is licensed under a Creative Commons Attribution 4.0 International license

3. The 28-day compressive strength was highest for RL2 (10% RHA + 2.5% lime) at 27.8 MPa, 5.3% higher than the control (26.4 MPa). Mixtures up to 17.5% total replacement met the target strength of 25 MPa.
4. Splitting tensile and flexural strengths followed the same trend, with maxima of 3.12 MPa and 4.45 MPa, respectively.
5. Water absorption decreased to 3.9% and the volume of permeable voids to 10.2% for RL2, indicating a denser matrix.
6. The optimum mixture in terms of cement efficiency was RL2, which saved 51.25 kg of cement per cubic meter (12.5%) while satisfying the strength requirement, supporting the use of RHA and lime for environmentally friendly concrete.

It is recommended that future work examine several lime dosages, longer curing ages, and durability indicators such as chloride penetration and sulfate resistance.

REFERENCES

Ashour, S. A., & Wafa, F. F. (1993). Flexural behavior of high-strength fiber reinforced concrete beams. ACI Structural Journal, 90(3), 279–287. https://doi.org/10.14359/4186

Behbahani, M. A. (2010). Assessment of hook end steel fibre as a substitute material in high performance concrete beam [Master's thesis, Universiti Sains Malaysia].

Beygi, M. H. A., Kazemi, M. T., & Nikbin, I. M. (2026). Evaluative response of hybrid steel fiber-reinforced high-performance concrete under static and fatigue bending after elevated temperature exposure. Composites Part B: Engineering, 295, 112234.

Fatimah, D., Susilo, D., & Bhayusukma, M. Y. (2021). Pengaruh penambahan serat baja ringan terhadap kuat tekan, kuat tarik dan kuat lentur pada beton mutu tinggi. Jurnal Teknologi Universitas Teknologi Yogyakarta.

Ferdosian, I., & Camões, A. (2021). Mechanical performance and post-cracking behavior of self-compacting steel-fiber reinforced eco-efficient ultra-high performance concrete. Cement and Concrete Composites, 121, 104071.

Ferdosian, I., Camões, A., & Jalali, S. (2021). Mechanical performance and post-cracking behavior of self-compacting steel-fiber reinforced eco-efficient ultra-high performance concrete. Construction and Building Materials, 281, 122587.

Huang, Z., Chen, L., & Liu, Y. (2024). Anisotropic behavior in the flexural properties of aligned steel fiber UHPC produced by electromagnetic field. Journal of Building Engineering, 88, 109142.

Johannes, D., Mangundap, K., Sugiharto, H., & Wijaya, G. B. (2021). Pengaruh penambahan serat baja 4D Dramix terhadap kuat tekan, tarik belah, dan lentur pada beton. Jurnal Teknik Sipil Universitas Kristen Petra, 15(2), 1–9.

Khalel, H. H. Z., Khan, M., Starr, A., Sadawi, N., Mohamed, O. A., Khalil, A., et al. (2025). Parametric study for optimizing fiber-reinforced concrete properties. Structural Concrete, 26(1), 88–110. https://doi.org/10.1002/suco.202300509

Kurniawan, A., & Himawan, L. (2025). Synergistic effects of steel fibers and silica fume on the workability, compressive strength, and flexural strength of concrete. Jurnal Teknik Sipil, 25(3), 2250–2257. https://doi.org/10.26418/jts.v25i3.89931

Kusnadi, A., & Setiawan, R. (2025). Karakteristik beton SCC dengan campuran abu sekam padi dan serat limbah scrap baja. Jurnal Teknik Sipil, 21(2), 145–156.

Lee, J., & Kim, S. (2009). An experimental study on structural behavior of steel fiber reinforced concrete. Journal of the Korea Concrete Institute, 21(5), 613–621.

This work is licensed under a Creative Commons Attribution 4.0 International license

Lim, T. Y., Paramasivam, P., & Lee, S. L. (1987). Behavior of reinforced steel-fiber-concrete beams in flexure. Journal of Structural Engineering, 113(12), 2439–2458. https://doi.org/10.1061/(ASCE)0733-9445(1987)113:12(2439)

Limbo, L. S., Kushartomo, W., & Hermawan, P. (2026). Pengaruh temperatur pembakaran terhadap sifat mekanik SCC berpenguat serat baja. Jurnal Mitra Teknik Sipil, 9(3), 215–228.

Liu, X., Chen, H., & Wang, Q. (2026). Polyvinylpyrrolidone-modified steel fibers for enhancing interfacial bonding and flexural properties of ultra-high performance concrete. Construction and Building Materials, 465, 140391.

Lolla, S., Oinam, R. M., Furtado, A., & Varum, H. (2025). Tensile strength and flexural behavior of steel fiber-reinforced concrete beams. Structural Concrete, 26(1), 501–530. https://doi.org/10.1002/suco.202400074

Meilita, S. (2026). Studi eksperimental beton mutu tinggi SCC dengan campuran SFWT (Steel Fiber Waste Tyre) [Undergraduate thesis, Universitas Andalas].

Nataraja, N., Nagaraj, T. S., & Basavaraja, S. B. (2013). Properties of steel fibre-reinforced concrete under compression. International Journal of Civil and Structural Engineering, 3(1), 1–12.

Ramasamy, N., Ganapathy, G., & Rajkumar, P. R. K. (2022). Flexural behaviour of high-performance concrete beams under cyclic loading conditions. Journal of Engineering Research, 2022, 1–12.

Sadrmomtazi, A., Tahmouresi, B., & Saradar, A. (2021). Physicomechanical behavior of high-performance concrete reinforced with recycled steel fibers from twisted cables in the brittle state Experimentation and statistics. Construction and Building Materials, 268, 121082.

Sahoo, D. R., & Sharma, A. (2014). Effect of steel fiber content on behavior of concrete beams with and without stirrups. ACI Structural Journal, 111(5), 1157–1166. https://doi.org/10.14359/51686821

Sharma, S. K., & Kumar, R. (2022). Studies on mechanical and fracture behaviour of fibre reinforced high performance concrete [Doctoral dissertation, Shodhganga].

Shi, K., & Gao, Z. (2025). Experimental and numerical study on flexural behavior of steel fiber reinforced high-strength concrete (SFRHC) beams. Scientific Reports, 15, 18338. https://doi.org/10.1038/s41598-025-02220-7

Sun, Y., Wu, Z., & Aslani, F. (2025). Flexural static and high-cycle fatigue behavior of steel fiber-reinforced ultra-high-performance concrete. Journal of Building Engineering, 102, 112890.

Thomas, J., & Ramaswamy, A. (2007). Mechanical properties of steel fiber-reinforced concrete. Journal of Materials in Civil Engineering, 19(5), 385–392. https://doi.org/10.1061/(ASCE)0899-1561(2007)19:5(385)

Tiberti, G., Germano, F., Mudadu, A., & Plizzari, G. A. (2018). An overview of the flexural post-cracking behavior of steel fiber reinforced concrete. Structural Concrete, 19(3), 695–718. https://doi.org/10.1002/suco.201700068

Wang, Y., Zhang, J., & Li, L. (2022). Positive effects of aligned steel fiber using the electro-magnetic field on flexural behavior of reinforced UHPC beams. In Proceedings of the 3rd International Conference on UHPC Materials and Structures (pp. 508–515).

Wu, D., Gao, W., & Feng, J. (2022). Experimental and theoretical study on flexural behavior of high strength concrete encased steel beams with steel fibers. Structures, 41, 1359–1368.

Yoo, D. Y., Yoon, Y. S., & Banthia, N. (2015). Predicting the post-cracking behavior of normal- and high-strength steel-fiber-reinforced concrete beams. Construction and Building Materials, 93, 477–485. https://doi.org/10.1016/j.conbuildmat.2015.06.006

This work is licensed under a Creative Commons Attribution 4.0 International license

Zhao, Y., Wang, X., & Li, H. (2025). Relationship between fiber dispersion, workability, and mechanical performance in self-compacting ultra-high performance concrete (SC-UHPC): An experimental and modeling study. Construction and Building Materials, 485, 141234.